ELSEVIER

Chemical Geology 202 (2003) 443–460

CHEMICAL GEOLOGY
INCLUDING
ISOTOPE GEOSCIENCE

www.elsevier.com/locate/chemgeo

Silicate weathering mechanisms determined using soil solutions held at high matric potential

F. Gérard*, J. Ranger, C. Ménétrier, P. Bonnaud

Institut National de la Recherche Agronomique (INRA), Unité Biogéochimie des Ecosystèmes Forestiers, Centre de Nancy, 54280 Champenoux, France

Received 26 September 2001; received in revised form 16 September 2002; accepted 19 December 2002

Abstract

We present evidence of surface-controlled and proton-promoted chemical weathering of primary silicates in a brown acidic soil (Vauxrenard, Rhône, France). We used aqueous silica (Si) in soil solutions held at high matric potential (180–1600 kPa), which are representative of solutions reacting with soil solids. Si concentration was well correlated with H^+ concentration and to a lesser extent with dissolved organic carbon (DOC), which showed a significant affect ($P<0.05$) only in the surface layer (0–15 cm). Significant negative linear relationships were obtained between log(Si) and pH at the profile scale, at each soil depth and for most sampling dates. We found no significant influence of soil temperature ($P>0.05$). Geochemical modelling showed that primary silicates dissolved under far-from-equilibrium conditions, and that organic ligands (modelled with a triprotic analogue) may have a weak but significant effect on the variations in log(Si) at the profile scale and at both 15–30 and 30–45 cm depths. Comparison of Si/Al ratios to literature data and observed soil mineralogy demonstrated that significant linear relationships found in the activity diagram between $\log[Al^{3+}]+3pH$ and $\log[H_4SiO_4^\circ]$ may not have been caused by the reversible formation of secondary Al–Si phases in the soil. Instead, the apparent trends may arise from relationships between log(Si) and pH and the control of Al-mobility by the reversible formation of Al-hydroxides in the vermiculite interlayer. All these results indicated that active, in situ chemical weathering of silicates may be surface-controlled and mostly proton-promoted. Mineralogy suggested that K-feldspar weathered much faster than albite and white mica, in contrast to the weathering gradient inferred from the mass balance between unweathered and soil material. This was certainly caused by differential changes in mineral reactive surfaces with time.

Keywords: Weathering; Silicates; Soil; Solutions; Matric potential; Modelling

1. Introduction

Knowledge of the mechanism controlling the chemical weathering rates of silicates in the field is important for several environmental issues. Acidification of soils and surface waters is closely connected to weathering, and this process also constitutes an important source of nutrients for plants over the long-term. The hydrolysis of silicates during rock weathering occurs via a sequence of mechanisms. The form of the kinetic expression depends on the nature of the rate-limiting mechanism. Thus, knowledge of the present-day, in

* Corresponding author. Tel.: +33-3-83-39-41-46; fax: +33-3-83-39-40-69.
E-mail address: gerard@nancy.inra.fr (F. Gérard).

0009-2541/$ - see front matter © 2003 Elsevier B.V. All rights reserved.
doi:10.1016/j.chemgeo.2002.12.001

situ rate-limiting mechanism is the first step toward the accurate calculation of chemical weathering rates using a reactive-transfer model.

It is well established that surface reactions control silicate weathering (i.e. surface-controlled dissolution) under laboratory conditions. One line of evidence is the decline in dissolution rates when the pH of the reacting solution increases (e.g. Nagy, 1995; Blum and Stillings, 1995; Drever and Stillings, 1997). Surface-controlled silicate dissolution rates become almost pH-independent at a pH greater than about 5 units. Below pH ~ 5, hereafter termed the acidic region, silicate dissolution mostly involves protons (H^+) as the reacting species and is said to be proton-promoted. Organic acids ranging from low molecular weight acid to humic substances may promote silicate weathering, depending on the pH and on the nature and concentration of organic substances (Bennett and Casey, 1994; Welch and Ullman, 1993, 1996; Ochs, 1996; Stillings et al., 1996; Drever and Stillings, 1997; Zhang and Bloom, 1999). Most of these authors report an increase in the promoting effect of low molecular weight organic acids with the pH of the reacting solution, as proton-promoted dissolution rate decreases and deprotonation of organic acids increases. Low molecular weight organic acids are typically more effective in accelerating silicate dissolution than larger molecules, such as fulvic acids (Zhang and Bloom, 1999) and humic acids (Ochs, 1996), possibly due to differences of carboxylic site densities and chelation efficiency (Drever and Vance, 1994). Furthermore, high molecular weight acids may even decrease the rate of silicate dissolution as pH increases (Ochs, 1996; Drever and Stillings, 1997). However, dissolved organic carbon (DOC) was generally found to enhance silicate dissolution under acidic conditions (Lundström and Öhman, 1990; Raulund-Rasmussen et al., 1998). This reveals the nature of the net effect on silicate weathering rates of the range of organic compounds present in natural samples.

Nevertheless, the exact nature of the rate-limiting mechanism remains unclear in the field. Weathering rates can be controlled by the diffusion of reacting or product species through microporous residual layers, amorphous or crystalline coatings stuck to mineral surfaces, and mineral micropores and mesopores (<50 nm) (e.g. Anbeek et al., 1994; Hochella and Banfield, 1995; White et al., 1996; Brantley, 1998; Nugent et al., 1998; Hodson, 1999). Soil minerals have generally been subjected to weathering agents over geological time spans, enabling residual layers and coatings to develop to a much greater extent than in the laboratory. The surface reactivity of minerals may decrease with exposure to weathering (Anbeek, 1993; Augusto et al., 2000). The well-known discrepancy between field and laboratory dissolution rate constants (e.g. Paces, 1983; Brantley et al., 1993; Swoboda-Colberg and Drever, 1993; White, 1995; White et al., 2001) gives further reason to wonder whether these differences are due to our inability to characterise the complexity of the dissolution mechanisms operating in natural systems or if dissolution mechanisms differ fundamentally between field and laboratory (White et al., 1996; Nugent et al., 1998).

The chemistry of soil solutions depends on the nature and intensity of active and in situ soil processes/mechanisms, and vice versa. Aqueous silica may be used as weathering rate indicator, as in the laboratory during experimental dissolution of silicates (e.g. Hellmann, 1994; Frogner and Schweda, 1998) and in some stream and river waters wherein its role as weathering rate indicator has also been pointed out when the stoichiometry of the overall weathering reactions is known (Meybeck, 1986; Drever and Zobrist, 1992; White and Blum, 1995; White et al., 1999). This research is aimed at investigating the active mechanisms controlling chemical weathering rates of soil silicates, using a certain type of soil solution collected from field samples. One may distinguish two main types of soil solutions according to the energy with which they are retained by solids, generally termed the matric potential (ψ). Leaching solutions circulate into interconnected macropores driven by the gravitational force, and solute species are transferred downward by advection. The remaining portion of the bulk soil water corresponds to "capillary" soil solutions, which are almost immobile as they are retained by capillary forces in narrower interconnected pores. Soil scientists used the field capacity to define the ψ value below which gravitational transfers may occur. The GRIZZLY database (Havenkamp et al., 1998) may be used to demonstrate that field capacity varies from about $\psi = 3-30$ kPa in most soils, depending on their texture and structure. Mass transfers between leaching and capillary solutions correspond to mixing processes, as they

occur via molecular diffusion and eventually via capillarity if ψ exceeds field capacity due to water loss by evaporation and evapotranspiration. Accordingly, the chemical properties of capillary and leaching solutions generally differ because of the differences in their residence time, implying different contact times with soil solids and some variations in the nature and intensity of the physical and biological processes. Capillary solutions are generally more concentrated in most solutes than leaching waters and their chemistry shows seasonal variations (Zabowski and Ugolini, 1990; Marques et al., 1996; Giesler et al., 1996; Ranger et al., 2001; Gérard et al., 2002). In our conceptual model, capillary solutions form a continuum in chemical terms because the impact of the evaporation and evapotranspiration processes is attenuated as ψ increases and, conversely, the influence of water–solid interactions on the chemical properties of capillary solutions increases with ψ (Fig. 1). Note that this is not only caused by the weakness of biological and physical processes but also by a weaker influence of molecular diffusion, since the diffusion distance for solutes released by water–solid interactions gets smaller as ψ increases. Therefore, we shall consider capillary solutions held at greater ψ values as most representative of the solution reacting with soil-forming minerals.

2. Materials and method

2.1. Field site and soil mineralogy

The soil studied is an acidic brown soil, classified as a 'Typic Dystrochrept' (USDA, 1998) or an Alocrisol (AFES, 1992), covered by a 45-year-old Douglas fir plantation (*Pseudotsuga menziesii* (Mirb.) Franco). The area studied is located in the Montagne des Aiguilettes in the Beaujolais (Rhône, France), at an altitude of about 750 m. The mean annual temperature is 7 °C and mean annual precipitation is ~ 1000 mm. Chemical properties of the soil, stand characteristics, ecological situation and nutrient dynamics have been discussed by Ranger et al. (1995), Marques et al. (1996) and Marques and Ranger (1997).

The mineralogy and chemical properties of the soil have also been comprehensively studied (Ezzaïm et al., 1997, 1999a,b). The bedrock is an Upper Visean volcanic tuff that has undergone hydrothermal alteration. Unweathered material contained about 45% quartz, andesine, albite and biotite phenocrysts (< 2 mm) and 55% devitrified groundmass. The devitrified volcanic glass consists of an association of quartz, andesine, albite, K-feldspar spherolites and biotite microcrysts (1–10 μm). The weathering gradient inferred from the mass balance between soil material (0–

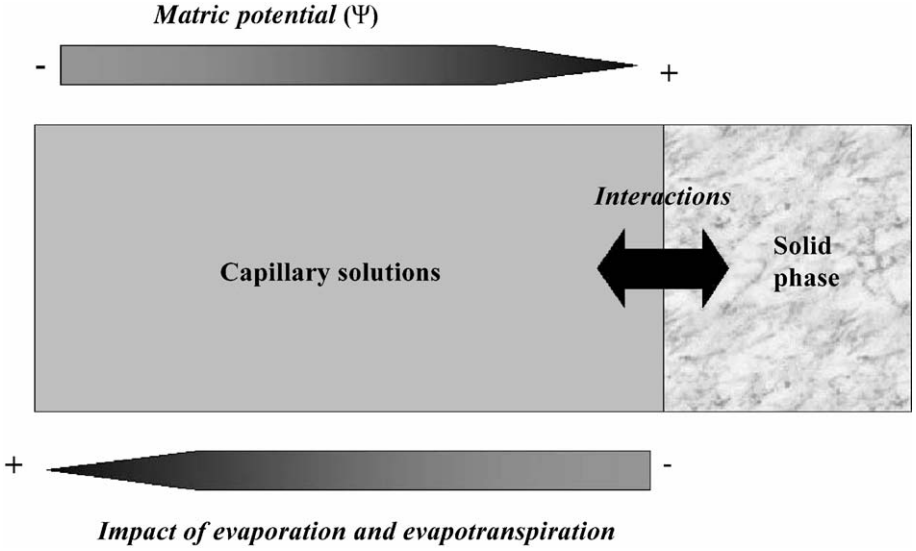

Fig. 1. Conceptual model used for the chemistry of capillary solutions.

1 cm) and the unweathered tuff was: quartz < K-feldspar < white mica < biotite < albite < andesine. Extensive Ca and Na depletion was observed in the soil material, corresponding to the almost complete dissolution of andesine and of ~ 77% albite (see Fig. 5 in Ezzaïm et al., 1999b). Meanwhile, the relative abundance of K-feldspar and white mica slightly increased by about 64% and 43%, respectively.

Scanning and transmission electron spectroscopy (SEM and TEM, respectively), and X-ray diffraction (XRD) have led us to identify kaolinite, hydroxy-Al interlayered vermiculites and interstratified vermiculite–biotite as secondary minerals. Small amounts of Si and Al were extracted by oxalate (Si_o and Al_o, respectively) from the fine earth fraction. Both oxalate and pyrophosphate released similar amounts of Al, proving that extractable Al was essentially organically bound. The very small value taken by the $(Al_p - Al_o)/Si_o$ ratio, with Al_p standing for Al extracted by pyrophosphate, further suggested that allophane or ITM were either absent or present in very weak quantities in the soil material (see Ezzaïm et al., 1999b).

2.2. Solution collecting technique

The centrifuge drainage method made it possible to collect capillary solutions corresponding to high matric potential (ψ) from soil samples collected in the field (e.g. Giesler and Lundström, 1993; Giesler et al., 1996). Here, a JOUAN KR4 22 centrifuge was used at room temperature ($T \sim 20$ °C). This apparatus permits the centrifugation of six soil samples of approximately 1600 cm^3 each placed in double bottomed polycarbonate tubes, consisting of an upper soil holding cup with a perforated base and a lower solution collecting cup. A stepwise procedure was adopted to extract the portion of capillary solutions corresponding to the highest matric potential. A first extraction was performed at 1000 rpm for 20 min, yielding capillary solutions corresponding to $\psi < 180$ kPa. The second step consisted of centrifuging the same soil samples for an additional 20-min period at 3000 rpm. Capillary solutions corresponding to a matric potential range of 180–1600 kPa were thereby obtained. In agreement with the above conceptual model for soil solutions, only capillary solutions corresponding to the higher matric potential range were retained in the present study and considered as the best representing of solutions reacting with soil minerals.

2.3. Soil sampling and solution chemistry

The soil samples were collected during five field campaigns from 1999 to 2000, in October and November 1999, February, May and October 2000. Extraction of capillary solutions in quantities commensurate with chemical analysis of major solutes (see below) is often prevented in the summer, because of excessively dry conditions. Thus, no sampling occurred in this season. Soil samples were collected at least two days after the last rainfall or snowmelt in order to minimise the replenishment of capillary solutions with new meteoritic water. Otherwise, the chemistry of capillary solutions could be misleadingly altered by leaching solutions given their different chemical properties, as discussed in Section 1.

Sampling points were selected to deal as well as possible with spatial variations in parameters controlling chemical weathering rates, especially mineral reactive surfaces. Samples were taken within three tree-free circular areas of approximately 2-m radius about 15 m apart. Three soil samples were taken from each collecting zone at three depth intervals (0–15, 15–30 and 30–45 cm) below the litter layer, corresponding to the A_1/A_P, A_P and A/(B) horizons, respectively. A stainless steel tube (length = 15 cm, diameter = 8 cm) was used and samples were immediately stored in plastic bags. The hole was partly refilled with litter, gravel, pebbles and uncollected soil material. Soil sampling locations were then marked to avoid being sampled at a later date. On average, about 72 h elapsed between field sampling and centrifugation in the laboratory. Samples were not refrigerated during transport. This time period covered field sampling, sample transportation and their centrifugation in the laboratory. Then, capillary solutions were immediately filtered after extraction through a 0.45-μm filter (GN-6 Metricel®, Pall) and pH was determined using a combination pH electrode (INGOLD-XEROLIT®) with a Mettler DL21 pH-meter. Total Si, Al, Ca, Mg, K, Na, Mn and Fe were analysed by ICP emission spectroscopy (JY 38+ spectrometer). DOC was measured with a SHIMADZU TOC 5050. Sulphate and fluoride were both analysed by ion chromatography (DIONEX DX 300).

Nitrate, ammonium and chloride were measured by colorimetry (TRAACS 2000). Soil temperature was measured at different depths with either in situ or portable temperature probes, depending on equipment availability.

2.4. Surface-controlled weathering rate equation

According to Lasaga (1995), a general surface-controlled rate expression as a function of the activity of reacting species in a non-isothermal system may be described by:

$$r = S\prod_i k_i[i]^{n_i} A\exp\left(\frac{-E_a}{RT}\right) \quad (1)$$

where r is the mineral dissolution rate (mol s^{-1} $kg_{H_2O}^{-1}$), S is the reactive surface of the mineral (cm^2 $kg_{H_2O}^{-1}$), k_i is the rate constant for the reaction involving the reacting species i (mol cm^{-2} s^{-1}), $[i]$ is the aqueous activity of reacting species i involved in the rate-limiting surface reactions, n_i is an experimental exponent, A is the pre-exponential factor, E_a is the apparent activation energy of the overall reaction (J mol^{-1}), R is the universal gas constant (8.31451 J mol^{-1} K^{-1}) and T is the Kelvin temperature.

By taking the logarithm of r with only H^+ and a given organic ligand (noted L) as the reacting species and by considering dissolved silica (Si) as weathering rate indicator, Eq. (1) becomes:

$$\log(\mathrm{Si}) = \log(Sk_{H^+}k_L A) + n_{H^+}\mathrm{pH} + n_L\log[\mathrm{L}] - \left(\frac{E_a}{2.303RT}\right) \quad (2)$$

Eq. (2) is valid if there is no change in the reaction mechanism with temperature and if species concentrations are not significantly altered by other reactions. It shows that log(Si) may be expressed as a linear function of pH, log[L] and T^{-1}, with slopes n_{H^+}, n_L and $-E_a/2.303R$, respectively. The slope n_{H^+} should have a negative value, in order to reproduce the decrease of the dissolution rate in the acidic range as pH increases. In contrast, the slope n_L can have either a negative or positive value depending on whether the given organic ligand slows or accelerates the dissolution rate.

2.5. Geochemical modelling

A number of variables and processes may obscure or yield spurious linear relationships between log(Si) and pH because of excessive dispersion of the data. Their influence may be identified by means of geochemical modelling, such as chemical affinity, A_r (with $A_r = -RT\ln[Q/K]$ with Q the ion activity product and K the thermodynamic equilibrium constant). Eq. (2) will be linear with respect to pH when $A_r \gg 0$ and therefore the influence of A_r on chemical weathering rates is weak. Note that this condition, generally termed as far-from-equilibrium, is also maintained in laboratory dissolution experiments in order to limit secondary phase precipitation. The standard Transition State Theory was used in this study to check whether soil silicates dissolved under far-from-equilibrium conditions or not when in contact with capillary solutions. Accordingly, the dissolution rate exhibits first order dependency with respect to A_r and may not be significantly altered if the A_r/RT ratio is greater than 3.

The formation of secondary aluminosilicates in soils can also affect silica mobility. Secondary aluminosilicates such as allophane and imogolite type materials (ITM) may form at relatively fast rates in acidic soils (hence their short range ordered nature) and may be kaolinite precursors (Steefel et al., 1990; Su et al., 1995; Lumsdon and Farmer, 1995). Accordingly, their formation occurs close to equilibrium and is thus influenced by their solubility (i.e. equilibrium-controlled reaction). It follows that this process can lead to mistaken linear relationships between log(Si) and pH because of the Al content of these phases (Si/Al ~ 0.5). The solubility of these phases depends directly and indirectly (i.e. through the activity of Al^{3+}) on the pH and should therefore increase non-linearly when the pH decreases. Because of the expected variability in the data, an apparent linear relationship between log(Si) and pH may be found, with a negative slope n_{H^+} as it would be with surface-controlled and proton-promoted silicate weathering (Eq. (2)).

Temperature changes induce solubility variations as well. The Van't Hoff expression (Eq. (3)) represents the influence of T on the equilibrium constant:

$$K = K_0\exp\left(\frac{-\Delta H_r}{RT}\right) \quad (3)$$

where ΔH_r is the standard enthalpy change for the reaction (or heat of reaction) over a given temperature range (J mol^{-1} K), K and K_0 are the equilibrium constants at a given temperature and at a reference temperature, respectively. A linear function of T^{-1} may be obtained by taking the logarithm of the Van't Hoff expression:

$$\log(K) = \log(K_0) - \left(\frac{\Delta H_r}{2.303RT}\right) \quad (4)$$

Assuming that the Si concentration was controlled by the equilibrium-controlled formation of ITM, log(Si) would be proportional to log(K). Since log(Si) may be falsely linearly related to the pH due to its effect on the solubility of ITM, as discussed above, one can write:

$$\log(\mathrm{Si}) \equiv \log(K_0) + n_{H^+}\mathrm{pH} - \left(\frac{\Delta H_r}{2.303RT}\right) \quad (5)$$

Comparison of Eq. (5) with Eq. (2) for the case of $n_L = 0$ clearly shows that a linear relationship might be obtained with the same dataset, though due to different Si-controlling processes. This demonstration can be extended to organic ligands as well, because Al speciation and thus the solubility of ITM may also be influenced by the organic ligand concentration through the formation of organo-Al complexes. A greater complexing influence of organic ligands would lower the activity of Al^{3+} and would thus increase the Si concentration needed to maintain an equilibrium with ITM, giving a positive value of n_L as expected in Eq. (2) should organic ligands significantly promote silicate weathering.

We have seen in the introduction that DOC in soil solutions encompasses a huge range of organic compounds of different molecular weight and functionality, which may have contrasting effects on silicate dissolution kinetics. DOC speciation is not yet readily determined and provisions for minimising the potential influence of organic ligands on field silicate weathering rates (i.e. $n_L[L] \rightarrow 0$ in Eq. (2)) were made to improve linear relationships between log(Si) and pH and T^{-1}. Studying mineral layers of an acidic forest soil where solution pH is mostly below 5, by definition, may satisfy this condition as data corresponding only to the acidic region wherein surface-controlled weathering may be mostly proton-promoted would be obtained. Nevertheless, since the influence of organic ligands may not be negligible, some simple models exist in the literature and may be used profitably to assess the organic ligand concentration for test purposes.

We incorporated one of these in the PHREEQC 2.0 hydrochemical computer program (Parkhurst and Appelo, 1999) used for calculating the equilibrium distribution of the aqueous species in capillary solutions and their chemical affinity for the dissolution of the primary silicates. We considered the triprotic analogue representation of the acid–base properties of the DOC collected in the Hubbard Brook Experimental Forest (Driscoll et al., 1994; Schecher and Driscoll, 1995). This approach permits the simulation of the complexation between dissolved Al and an analogue organic ligand, L, having a mean site density, m, equal to 0.055 mol site/mol carbon (Driscoll et al., 1994). Boudot et al. (1994) obtained acceptable agreement between this model and experimental values of Al speciation in solutions collected from forested acidic soils located in the Vosges mountains (N.E. France). More recently, Boudot et al. (2000), Maitat et al. (2000) and Gérard et al. (2001) used this model to simulate Al speciation in acidic soil porewaters collected from a number of other forested acidic soils. The question of the relative validity of the triprotic analogue representation of the acid–base properties of DOC was raised by a recent research showing that low molecular weight and higher molecular weight-acids in acidic forest soils exhibited similar acid–base properties (Bergelin et al., 2000).

The origin the thermodynamic data used in PHREEQC 2.0 for mineral and inorganic aqueous species has been thoroughly discussed in Gérard et al. (2001). Natural imogolite (Zysset et al., 1999) was added to the initial database in order to encompass the wide range of log(K) values proposed in the literature for ITM. Upper and lower solubility boundaries for ITM were defined by the maximum and the minimum log(K) values (i.e. log(K) plus and minus the standard deviation) for proto-imogolite sol (PI) and natural imogolite. Soil vermiculites were not considered in the thermodynamic database because of the uncertainties with respect to the stability of interstratified clays. Furthermore, there was a lack of data on the distribution of Al between interlayer, octahedral and tetrahedral sites, which meant that it was not possible to

calculate a mean structural formula (see Ezzaïm et al., 1999b). Conversely, the thermodynamic equilibrium constant for white mica, $K_{0.94}(Mg_{0.19}Fe(II)_{0.14}Al_{1.71})Al_{0.73}Si_{3.27}O_{10}(OH)_2$ (see Ezzaïm et al., 1999b), was estimated using an ideal solid solution model (Tardy and Fritz, 1981) according to Eq (6).

$$\log(K_m) = \sum_j x_i \log(K_i) + \sum_j x_i \log(x_i) \quad (6)$$

where K_m is the equilibrium constant of the ideal solid solution m, j is the number of end-members i required to model the solid solution, x_i is the mole fraction of the end-member i in the solid solution m and K_i is the thermodynamic equilibrium constant for the end-member i. Three end-members available in the database were used (muscovite, annite and Mg-phlogopite).

The primary mineral biotite was not considered in this study. Our choice was supported by the very great extent of the transformation of biotite to secondary clays (vermiculite and interstratified vermiculite–biotite), compared to the relatively small amount of biotite within the unaltered tuff (Ezzaïm et al., 1999a,b).

2.6. Statistics

All the statistics were computed using the program SAS version X81 for UNIX (SAS Institute). The first set of tests concerned general statistics of the measured variables relevant to the present work, i.e. Si and H^+ concentrations, DOC and soil temperature. A preliminary study of correlations between these variables was made by means of a factor analysis (PCA, two factors). Then variance analysis (ANOVA), followed by multiple comparisons (Student–Neumann–Keuls) whether necessary (i.e. null hypothesis rejected), were used in order to get the statistical significance of the previous correlations and to study the influence of soil depth and sampling depth on Si concentration. In a second step, attempts to obtain significant relationships between log(Si), pH and T^{-1} and the organic ligand term in Eq. (2) were made by multiple linear regression analysis. In a first step, statistical analysis was made between measured variables only, i.e. between log(Si), pH and T^{-1}. Thereafter, the organic ligand term was included in the multiple linear regression analysis for test purposes.

3. Results

3.1. General statistics, factor analysis and ANOVA

Capillary solutions were extracted from more than 100 soil samples by centrifugation and analysed ($N=114$). Measured pH never exceeded 5 units and ranged from 3.8 to 4.9 exhibiting a standard deviation (S.D.) of 0.21. Si concentrations ranged from 4.2 to 19.3 mg l^{-1}. Soil temperatures ranging from $T=2$–12 °C were measured when soil samples were collected. DOC ranged from 10 to 74 mg l^{-1}.

Factor analysis done with the variables DOC, Si and H^+ concentrations, and T showed that Si concentration was tightly correlated with H^+ concentration, through the first principal component (Fig. 2). Soil temperature was poorly correlated with the other variables, especially Si concentration. A better correlation was found between Si concentration and DOC. The statistical significance (i.e. P-value) of such correlations was studied by means of variance analysis (ANOVA), by taking into account the plausible influence soil depth and sampling date on Si concentration (taken as factors). The variables H^+ concentration, DOC and T were considered/tested as covariates of Si concentration. The relationships between Si and both H^+ and DOC were highly significant ($P<0.0001$), while there was a lack of significant influence of T. Sampling date, unlike soil depth, exhibited a significant influence on Si concentration but we also obtained a highly significant interaction between soil depth and sampling date. This required additional ANOVA using data subsets corresponding to the different sampling dates (regardless of soil depth) and to the different soil depths (regardless of sampling date). By doing so, a unique factor may be considered in ANOVA, either soil depth or sampling date. In the first case, soil depth significantly affected Si concentration except for the subset of data corresponding to February 2000. A significant correlation between Si and H^+ concentrations prevailed for all sampling dates. In contrast, there was a lack of significant affect of T on Si concentration in all the cases (i.e. whatever the sampling date), as well as for DOC with an exception in October 2000. Multiple comparisons showed that the maximum Si concentration was reached in the surface layer (0–15 cm), corresponding to Si ~ 15 mg l^{-1} compared to an average of about 8 mg l^{-1} at the other depths. Within

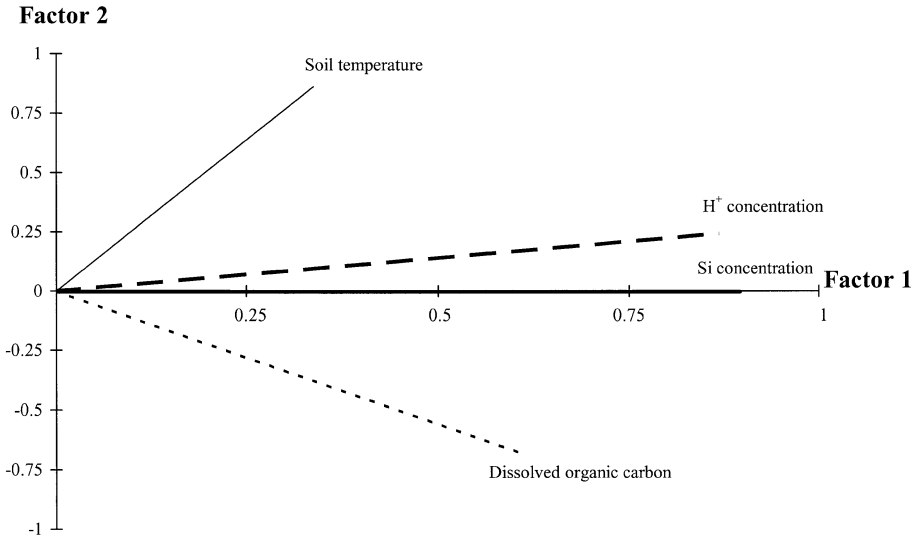

Fig. 2. Result of the factor analysis (PCA, two factors) using the measured silica, H^+, dissolved organic carbon concentrations and soil temperature.

data subsets corresponding to the different soil depths, sampling date always significantly affected Si concentration. The maximum Si concentration was reached in May and/or October 2000 ($\sim 15-10\ mg\ l^{-1}$), depending on the soil depth. Meanwhile, Si concentration was well correlated with H^+ at each soil depth (i.e. in all the data subsets), while the correlation with DOC was only significant in the surface soil layer.

3.2. Log(Si)–pH–T^{-1} relationships

Attempts to establish significant relationships between log(Si) and pH and T^{-1} were first made by multiple linear regression analysis of Eq. (2), without the term representing organic ligands. The whole set of data was first used regardless of the soil depth interval and sampling date. Such a scale (hereafter referred to as the profile scale) appeared the most suitable to minimise the distorting influence of data variability due to uncontrolled variables and processes (reactive surfaces, mass transfers, organic ligands, etc.) as it provided the greatest number of data. Moreover, results may be indicative of the Si-controlling process at the soil profile scale. By doing so, a highly significant linear relationship ($P<0.0001$) was established between log(Si) and pH at the profile scale (Fig. 3), whereas no significant influence of the temperature term (i.e. T^{-1}) was found. This was consistent with the absence of significant correlation between soil temperature and Si concentration found in the previous section. The slope, n_{H^+}, of the relationship between log(Si) and pH was equal to -0.47 (S.E. = 0.05). The coefficient of determination, R^2, indicated that about 43% of the variability in log(Si) concentration was controlled by pH.

Then, multiple linear regression analysis was done with the same data subsets defined in the previous section. First, data from the different soil depth intervals were considered. A highly significant linear relationship between log(Si) and pH prevailed at 0–15 cm depth ($N=39$) and there was still no significant influence of the temperature term (Table 1). Beneath the upper soil mineral layer, at the 15–30 and 30–45 cm depths, there was a persistent lack of influence of the temperature term in Eq. (2) on log(Si). Significant linear relationships between log(Si) and pH were still calculated (see Table 1), though to a lesser extent than at either the profile scale or surface layer interval, suggesting that the control of log(Si) by pH was apparently weaker than in the upper soil layer.

Multiple linear regressions for data subsets corresponding to each sampling date also showed a lack of significant influence of soil temperature on log(Si). Significant relationships between log(Si) and pH were

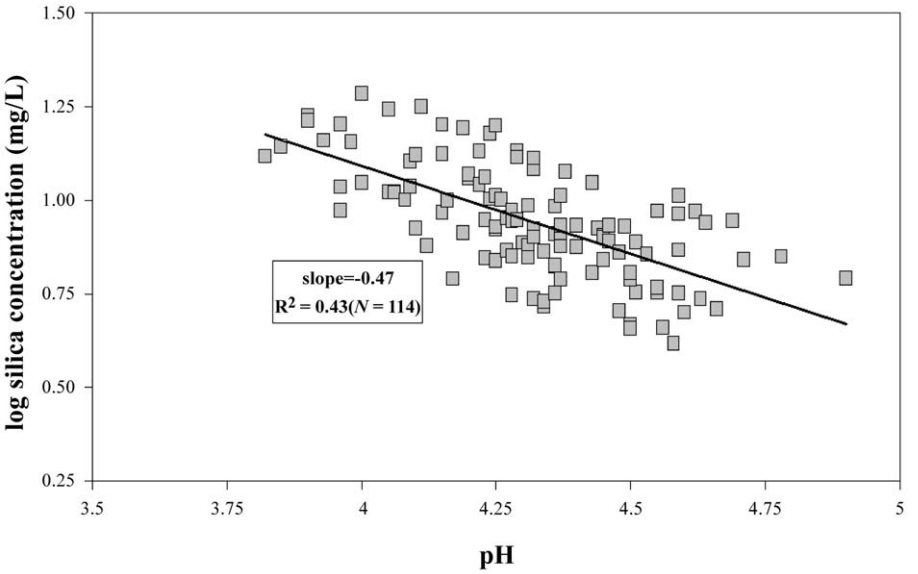

Fig. 3. Linear relationship between the logarithm of the silica concentration and the pH of capillary solutions at the soil profile scale.

obtained for all sampling dates except for October 2000 (Table 2).

3.3. Modelling

A temperature constraint is required for geochemical modelling since this variable affects the stability of aqueous species and minerals. Statistical analysis failed to reveal a significant effect of T on Si concentration (note that plausible explanations for this result are discussed in Section 4.4). The absence of correlation between Si concentration and T suggests that a single temperature value could be reasonably used to calculate aqueous speciation and chemical affinities of capillary solutions. In the absence of an obvious and relevant single temperature value, the following calculations were done at $T = 25$ °C because it corresponds to the standard condition at which thermodynamic parameters used by the model are better known. Therefore, setting $T = 25$ °C should minimize modelling errors.

It can be seen in Fig. (4) that the A_r/RT ratio in capillary solutions for the dissolution of albite and white mica was mostly higher than the threshold value

Table 1
Slope (n_{H^+}), coefficient of determination (R^2), significance (P) and number of data (N) for the relationships between log(Si) and pH calculated with the data subsets corresponding to each soil depth interval

Soil depth interval (cm)	n_{H^+}	R^2	P	N
0–15	−0.54 (0.09)	0.49	****	39
15–30	−0.30 (0.09)	0.24	**	39
30–45	−0.46 (0.12)	0.29	***	36

****$P < 0.0001$, ***$0.0001 < P < 0.001$, **$0.001 < P < 0.01$, *$0.01 < P < 0.05$, ns = $P > 0.05$.
Values in parentheses are the standard error (S.E.) associated with the slope.

Table 2
Slope (n_{H^+}), coefficient of determination (R^2), significance (P) and number of data (N) for the relationships between log(Si) and pH calculated with the data subsets corresponding to each sampling date

Sampling date (month–year)	n_{H^+}	R^2	P	N
10–99	−0.42 (0.12)	0.41	****	19
11–99	−0.73 (0.09)	0.71	****	27
02–00	−0.25 (0.12)	0.16	*	25
05–00	−0.35 (0.08)	0.48	***	23
10–00	ns	0.15	ns	20

****$P < 0.0001$, ***$0.0001 < P < 0.001$, **$0.001 < P < 0.01$, *$0.01 < P < 0.05$, ns = $P > 0.05$.
Values in parentheses are the standard error (S.E.) associated with the slope.

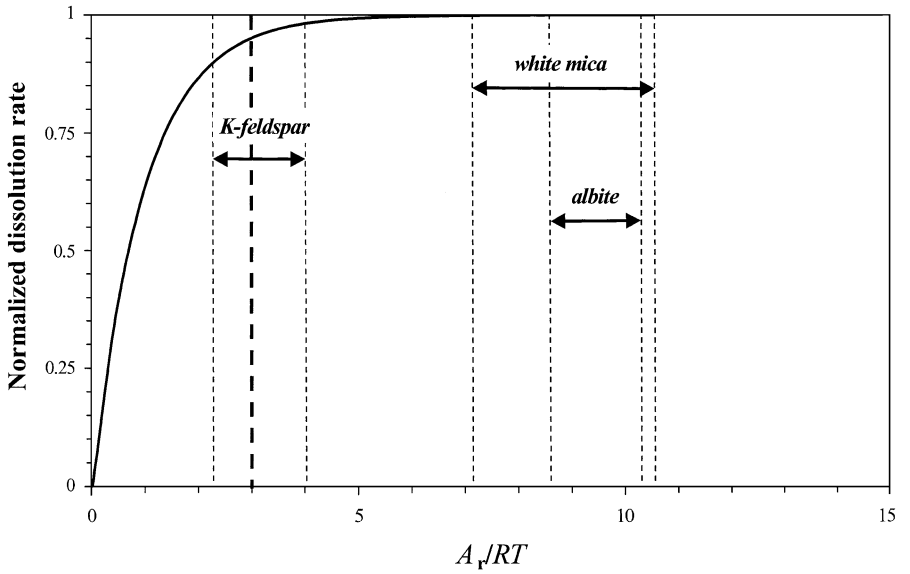

Fig. 4. Normalized dissolution rate (i.e. dissolution rate divided by far-from-equilibrium dissolution rate) plotted as a function of the chemical affinity term (A_r/RT), at $T=25$ °C. Thin dashed lines correspond to the range of A_r/RT ratios calculated for primary minerals (mean value ± standard deviation). The thick dashed line stands for the threshold value of 3 for the A_r/RT ratio given by a first order dependency of the dissolution rate, according to the standard Transition State Theory. Below this limit ($A_r/RT<3$), the dissolution rate is significantly reduced (i.e. by over 5%) by the chemical affinity of the reaction.

of 3 specified by the Transition State Theory. Mean A_r/RT values for albite and white mica were 9.42 (S.E. = 0.08) and 8.80 (S.E. = 0.16), respectively, implying that their dissolution is unaltered by chemical affinity (i.e. normalized rate equal to 1). The mean value of the A_r/RT ratio for K-feldspar was 3.11 (S.E. = 0.08) and thus overlaps the threshold value. Accordingly, K-feldspar dissolution rate may be decreased by 10% (i.e. normalized rate of 0.9) due to the effect of chemical affinity.

The thermodynamic state of capillary solutions regarding equilibrium with secondary phases in the Al–Si system was studied by means of the relevant activity plot of $\log[Al^{3+}]+3pH$ vs. $\log[H_4SiO_4^\circ]$ (Fig. 5). Capillary solutions were greatly over-saturated with respect to poorly crystallized kaolinite, certainly the best proxy for the kaolinite identified in this soil (Section 2.1). Solutions were close to equilibrium with respect to natural imogolite at low activities in orthosilicic acid (lower than about $10^{-3.5}$), but this phase has not been observed in this soil. A linear regression analysis of all the data gave a slope of −1.45 (S.E. = 0.14), corresponding to the Si/Al ratio of a hypothetical secondary phase, with an R^2 coefficient equal to 0.47 ($P<0.0001$). Speciation calculations indicated that most (~ 99%) dissolved Si was present as $H_4SiO_4^\circ$, in agreement with measurements done by van Hees et al. (2000) in acidic soil solutions. Accordingly, the linear regression between $\log[Al^{3+}]+3pH$ and log(Si) gave an R^2 coefficient almost unchanged, equal to 0.40, indicating that about 40% of the variability in log(Si) may be controlled by the relatively fast and reversible formation (i.e. equilibrium-controlled) of a hypothetical Al–Si compound. The same calculations were made with data subsets for each soil depth interval and sampling date (Table 3). Significant linear relationships were obtained except for data from October 1999. Significant calculated values of the slope were scattered and indicated that a hypothetical compound with a Si/Al ratio ranging from about 0.5 to 2.34 may control from 79% of the variability in log(Si) at most (in October 2000) to 17% at least (at 30–45 cm depth).

The second step of the multiple linear regression analysis of the data using Eq. (2) in its full form was to test the influence of organic ligands on aqueous silica mobility. As discussed previously, a very simplified approach was adopted, based on a triprotic analogue representation of the acid–base properties of DOC.

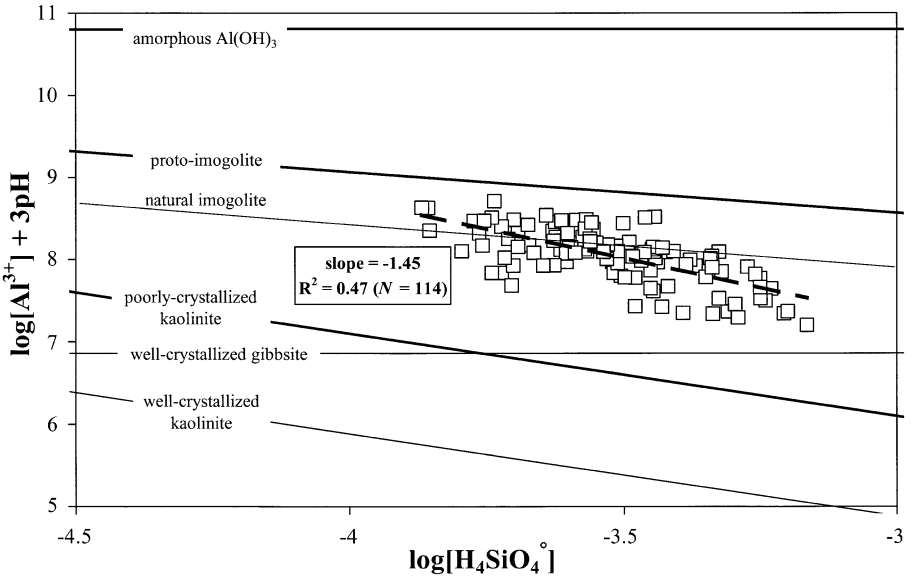

Fig. 5. Activity diagram for capillary solutions at the profile scale (T=25 °C) showing a significant linear relationship between the logarithm of the activity of orthosilicic acid, log[H_4SiO_4°], and the activity term for Al^{3+}(log[Al^{3+}]+3pH).

The outputs of the calculation were used to generate an organic ligand concentration as follows:

$$(L) = (H_2L^-) + 2(HL^{2-}) + 3(L^{3-}) \quad (7)$$

where the species L stands for the triprotic organic analogue, expressed in terms of molar concentration (mol l^{-1}), and (L) is the equivalent organic ligand concentration (mol l^{-1}).

Table 3
Absolute value of the slope (Si/Al), coefficient of determination (R^2), statistical significance (P) and number of data (N) for the linear relationships between log[Al^{3+}]+3pH and log[H_4SiO_4°] calculated with different subsets of data corresponding to the different soil depth intervals and sampling dates (values in parentheses are the standard error (S.E.) associated with the slope)

Data subsets	Si/Al	R^2	P	N	$R^{2a}_{tot.}$	$P^{b}_{tot.}$
0–15 cm	1.52 (0.24)	0.51	****	39	0.48	****
15–30 cm	1.18 (0.26)	0.36	****	39	0.23	**
30–45 cm	0.72 (0.21)	0.25	**	36	0.17	*
Oct. 1999	ns.	0.12	ns	19	0.05	ns
Nov. 1999	1.14 (0.29)	0.37	***	27	0.27	**
Feb. 2000	0.81 (0.32)	0.22	*	25	0.20	*
May 2000	1.70 (0.46)	0.40	**	23	0.38	**
Oct. 2000	2.09 (0.25)	0.80	****	20	0.79	****

****$P<0.0001$, ***$0.0001<P<0.001$, **$0.001<P<0.01$, *$0.01<P<0.05$, ns=$P>0.05$.

[a] Coefficient of determination of the linear relationships between log[Al^{3+}]+3pH and log(Si).

[b] Significance of the linear relationships between log[Al^{3+}]+3pH and log(Si).

Accounting for the organic ligand term confirmed the lack of influence of the temperature term. Organic ligands were found to have a significant effect on log(Si) at the profile scale. The corresponding partial R^2 coefficient was equal to 0.09 ($P<0.0001$) and the regression parameter (n_L) took a positive value equal to 0.16 (S.E.=0.03). The regression parameter of the pH term, n_{H^+}, was then equal to −0.50 (S.E.=0.05). The partial R^2 value for the relationship between log(Si) and pH was unaltered compared to the statistical analysis first made without taking into account the organic ligand term (see Section 3.2). The model R^2 coefficient (i.e. the sum of the partial R^2 value for pH and organic ligand terms) was equal to 0.52.

Making distinction between each soil depth interval, there was a lack of significant effect of organic ligands on log(Si) in capillary solutions from the surface layer (0–15 cm). However, a significant influence was found in the deeper soil depth intervals. At 15–30 cm depth, a partial coefficient of determination of about 0.19 (P=0.0015) was obtained for the organic ligand term, with n_L=0.23 (S.E.=0.07). The regression parameter n_{H^+} became equal to −0.52 (S.E.=0.10). At 30–45 cm depth, the influence of

organic ligands appeared to be weaker but was still significant ($P = 0.01$), with $n_L = 0.27$ (S.E. = 0.10) and a partial R^2 value of 0.12. The newly calculated value of n_{H^+} was -0.76 (S.E. = 0.16). Multiple linear regressions applied to data subsets corresponding to the different sampling dates regardless of soil depth did not show a significant influence of organic ligands.

4. Discussion and conclusions

4.1. Possibility of control by secondary phases

Several results showed a great deal of uncertainty whether there is a significant control of Si concentrations by the fast reversible formation of secondary phases, inferred from the establishment of linear relationships between $\log[Al^{3+}] + pH$ and log(Si) (see Section 3.3). In particular, Si/Al ratios of the hypothetical Si-controlling solids were generally inconsistent with these reported for allophane and ITM. ITM, which are well-defined allophane compounds, typically exhibit a Si/Al ratio of 0.5 (Wada, 1989; Su et al., 1995; Lumsdon and Farmer, 1995). According to Wada (1989), siliceous allophane-type compounds with a Si/Al ratio greater than one have not been isolated in soils. Consistent with this, soil mineralogy did not reveal the presence of such secondary phases, either by direct measurement (XRD, SEM and TEM observations) or by chemical extraction of short range ordered to amorphous products present in the soil material (see Section 2.1). Note that the role of Si–Al colloid species observed in acidic forest soil solutions and exhibiting a wide composition range (Xu and Harsh, 1993 and references cited therein) do not seem very persuasive to date, because of the uncertainty surrounding the possibility of these species being in or close to a thermodynamic equilibrium state with soil solutions. Dietzel (2000, 2001) measured the occurrence of relatively stable polysilicic acids released by dissolving silicates, which further combined with soluble Al to form Al–Si polymers of greater stability. This appeared to be inconsistent with their reversible formation in natural soil solutions.

We believe that significant relationships between $\log[Al^{3+}] + 3pH$ and either $\log[H_4SiO_4^\circ]$ or log(Si) stem from the concomitant effect of the control of Si by surface-controlled chemical weathering of silicates and two other processes widely recognized as controlling Al-mobility in forest soils, notably in the absence of allophane-type materials. The mixing up of these processes may explain why relationships drawn up over the activity diagram closely mapped linear relationships between log(Si) and pH (see Section 3.2). For example, the best fit was obtained with both relationships at the surface soil depth interval and became markedly weaker as soil depth increased.

It is widely recognised that the major Al-controlling processes in acidic soils are the reversible formation of hydroxy-Al compounds and the adsorption of soluble Al on soil organic matter (Bloom et al., 1979; Cronan et al., 1986; Dalghren and Walker, 1993; Berggren and Mulder, 1995; Simonsson and Berggren, 1998, Monterroso and Macías, 1998). The control of soluble Al by exchange reactions with soil organic matter convincingly explained linear relationships between $-\log[Al^{3+}]$ (i.e. pAl) and pH in solutions undersaturated with respect to the type of Al-hydroxide identified in the soil material. The relative importance of these two Al-controlling processes depends on both the pH and the organic matter content of the soil. In organic horizons, exchange reactions with soil humic substances may exert an influence at pH < 5.2 (Cronan et al., 1986). In mineral organic horizons, wherein organic matter content ranged from 1.9 to 0.68 wt.% (Rosenlund soils, in southernmost Sweden), Berggren and Mulder (1995) found a limit at about pH = 4.1.

Consistent results were found in this study regarding the presence of Al-hydroxides in the interlayer of soil vermiculites and the very low organic carbon content of this soil at the studied depth intervals (see Ezzaïm et al., 1999b). Solutions at the profile scale were supersaturated and under-saturated with respect to well-crystallized gibbsite and amorphous $Al(OH)_3$, respectively (Fig. 6). Throughout the measured pH range, most of the data were found to be close to equilibrium with respect to interlayered Al-hydroxides in vermiculites determined by Dalghren and Walker (1993). A highly significant linear relationship was found between pAl and pH over the entire pH range ($R^2 = 0.72$, $P < 0.0001$, $N = 114$), with a slope (ratio Al/OH) of 2.21 (S.E. = 0.13). Although significantly below the value of 2.7 reported by Dalghren and Walker (1993), this value was consistent with the Al/OH ratio determined for Al-hydroxides formed in vermiculite interlayers, which ranges from 2 to 2.8 (Barhisel and

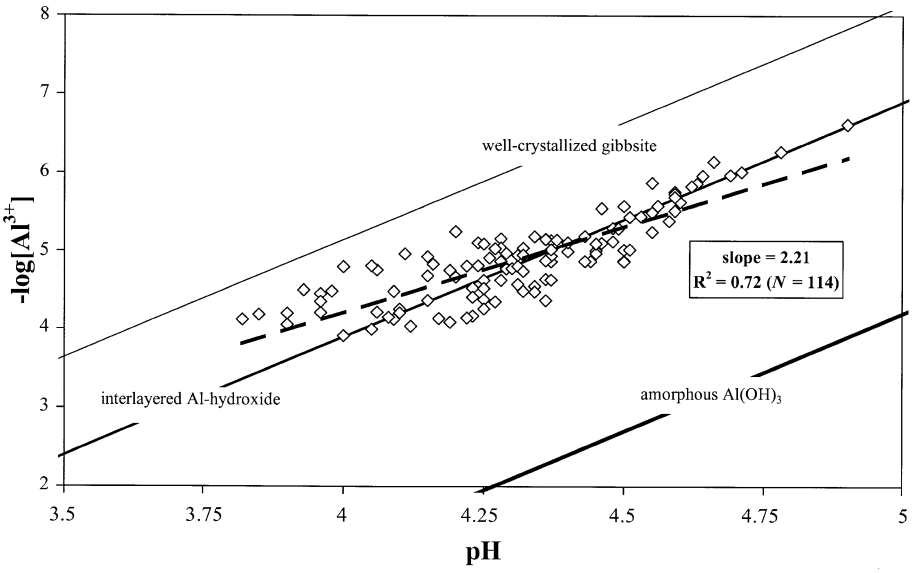

Fig. 6. Activity diagram for capillary solutions at the profile scale ($T = 25$ °C) showing a significant linear relationship between the negative of the logarithm of the activity of Al^{3+}, $-\log[Al^{3+}]$, and the pH.

Bertsch, 1989; Monterroso and Macías, 1998). Using only data at pH>4.1 would give better results regarding the control of Al mobility by Al-hydroxides (Berggren and Mulder, 1995). By doing so, the coefficient of determination slightly increases to 0.73 ($P < 0.0001$) and the slope increases (Al/OH = 2.70 ± 0.17) to the value determined by Dalghren and Walker (1993). Note that the consistency of our results with those in the literature also support the relatively good validity of our thermodynamic database for acidic forest soils.

4.2. Surface-controlled and dominating proton-promoted chemical weathering

If the previous arguments for the absence of significant Si-controlling phases are correct, significant relationships between log(Si) and pH may therefore be indicative of active surface-controlled chemical weathering of soil silicates. Geochemical modelling indicated that soil capillary solutions are far-from-equilibrium with respect to primary silicates, which is a prerequisite for the establishment of linear relationships between log(Si) and pH involved in the chemical weathering of primary silicates. Furthermore, our results also suggest that chemical weathering in this soil is weakly enhanced by organic ligands and is promoted by H^+. If this were not the case, it is uncertain whether significant relationships between Si and H^+ (see Section 3.1) and log(Si) and pH (see Section 3.2) could be obtained while disregarding the influence of organic ligands on chemical weathering. Consistent with this, multiple linear regression analysis with a term representing organic ligands (by means of an analogue organic ligand, L) gave partial R^2 coefficients that were either too low to ensure significant results or much lower than the pH term (see Section 3.3). In addition, it was calculated that the analogue organic ligand only had a significant affect on the variability in log(Si) below the surface soil layer. Additional ANOVA focusing on the variations in H^+ concentration as a function of soil depth indicated that capillary solutions collected at 15–30 and 30–45 cm depth were less acidic than in the surface soil layer (mean pH ~ 4.14 compared to ~ 4.32 units beneath). This result supports the validity of the triprotic analogue model for studying the relative contribution of low molecular weight organic acids vs. protons in the mechanisms of silicate weathering in acidic forest soils (see Section 1). It is interesting to outline the divergence between the apparent influences of the analogue ligand on Si concentration, calculated with Eq. (2), and that of DOC unravelled by a factor

analysis and ANOVA. Possibly DOC may be a better proxy for the effect on silicate dissolution of larger organic molecules, such as fulvic acids, which usually constitute the major fraction of DOC (van Hees et al., 2001 and references therein) and have been recognized in the laboratory for their greater accelerating effect as pH decreases (see Section 1).

4.3. Assessing the active weathering sequence

As our results indicated that Si mobility in capillary solutions may be controlled by surface-controlled and mostly proton-promoted weathering, the calculated n_{H^+} value corresponded to the order of the overall weathering rate of soil primary silicates with respect to pH. In the laboratory, the pH dependency of silicate weathering is studied by utilizing dissolution rates normalized to a surface area, S, as it can be measured unlike in natural systems. Nevertheless, an analogy between values of n_{H^+} measured in the laboratory and those calculated here from field samples seemed to be reasonably valid. Actually, one must assume that variations in S in this soil did not show a systematic trend with the solution pH. Variations in S are most likely contributing to data dispersion.

Both albite and K-feldspar typically exhibit pH dependency of about -0.5 in the acidic region (see review by Blum and Stillings, 1995). The pH dependency for the white mica present in our soil has not been studied in the laboratory. Therefore, we compare with muscovite as a proxy. Muscovite typically exhibits much lower pH dependency than alkali-feldspars. Kalinowski and Schweda (1996) obtained $n_{H^+} = -0.14$ to -0.20 at $T = 25$ °C. Nagy (1995) reported n_{H^+} values for muscovite that range from -0.10 to -0.08 under similar temperature conditions and pH. We have seen previously that biotite was extensively transformed to secondary products and was almost absent in the soil material. Therefore, this sheet silicate was excluded from the list of potential Si-controlling primary silicates. Comparisons between calculated n_{H^+} values, including error bars spanning a symmetric confidence interval of 95% (Webster, 2001), and those measured in the laboratory under similar conditions suggest that alkali-feldspars weathered significantly faster than white mica (Fig. 7). Values of n_{H^+} corresponding to the different groups of data were markedly outside the range of laboratory values for muscovite and overlapped the laboratory value for alkali-feldspars, whether the weak simulated influence

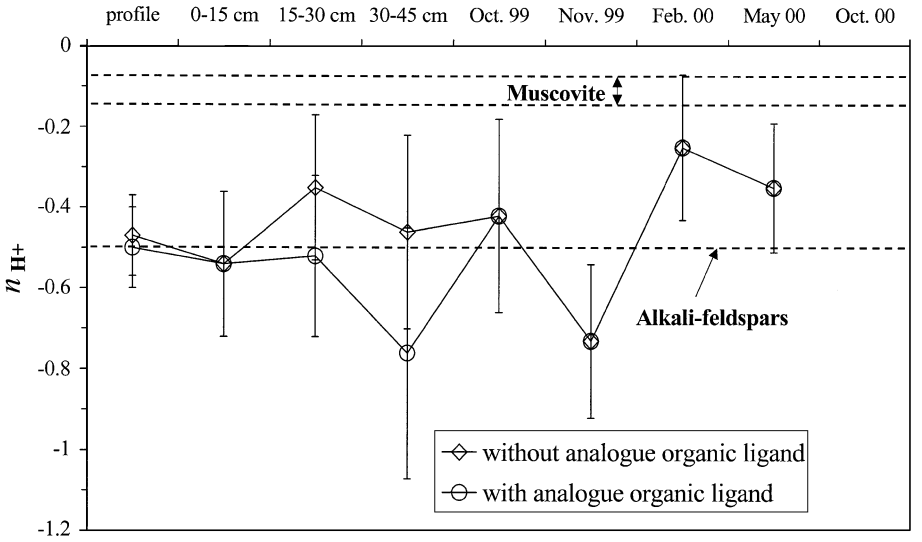

Fig. 7. Values of the linear regression parameter n_{H^+} (i.e. the slope of relationships between log(Si) and pH) calculated with different sets of data either considering the influence of organic ligands (open circles) or not (open diamonds). Error bars span a symmetric confidence interval of 95% of the mean value. Thick dashed lines represent the n_{H^+} values measured in the laboratory for primary minerals.

of organic ligands was taken into account or not. More variable results were obtained by distinguishing each collecting date (see Fig. 7), certainly due to the smaller number of samples involving a larger hindering influence of uncontrolled variables and processes. For example, error bars in February 2000 suggest that the control of Si concentration by white mica is possible, and the range of n_{H^+} corresponding to November 1999 was inconsistent with both alkali-feldspar and white mica weathering. But, at the profile scale, where the larger number of samples furnished a better statistical definition of the relationship between log(Si) and pH (i.e. smaller SE and confidence interval), the calculated n_{H^+} value was clearly consistent with alkali-feldspar dissolution in the laboratory.

This approach clearly suggest that the historical weathering sequence may still prevail, as it was found that albite should have been weathered much more intensively than muscovite (see Section 2.1). However, Ezzaïm et al. (1999b) found that the relative abundance of albite has decreased by about 77% in the soil material compared to the unweathered tuff, whereas that of K-feldspar has increased by 63%. Such an intensive reaction over the long term has certainly led to a greater decrease in the reactive surface (S) for albite than for K-feldspar and perhaps a proportional change in relative weathering rates. The possibility of a higher weathering rate for K-feldspar compared to albite seems reasonable, as the dissolution rate constants in the acidic region (k_{H^+}) are similar (see review in Blum and Stillings, 1995). Estimating the reactive surface area of weathered silicates in the soil material can confirm such an important finding. Besides, attempts to establish significant linear relationships between Si concentration and potassium concentration, for K-feldspar, and sodium concentration for albite, proved to be unsuccessful. This indicated that processes other than weathering controlled alkaline element concentration, perhaps ion exchanges and solute uptake by roots or litter degradation.

The empirical equation for mineral reactive surfaces included in the PROFILE computer programme (Sverdrup and Warfvinge, 1995) may be used for this purpose. This function gives the total reactive surface of a soil per unit of bulk soil volume ($S_{tot.}$ in $m^2\ m^{-3}$). Input parameters are the main size fractions of the soil material, soil density and density of the solid phase. Using data from Ezzaïm et al. (1999b) for size fractions with a soil density of 0.8 g cm^{-3} and a solid phase density of 2.7 g cm^{-3}, we obtained $S_{tot.} \sim 0.75\ m^2\ m^{-3}$, regardless of the soil depth interval, from which we calculated $S \sim 60\ cm^2\ m^{-3}$ for albite compared with up to 420 $cm^2\ m^{-3}$ for K-feldspar.

4.4. On the absence of a temperature effect on Si concentration

The time elapsed at $T = 20$ °C, from the moment at which samples were collected in the field to when solutions were extracted in the laboratory, may be long enough to allow a fast reaction to equilibrate with the new temperature conditions. Accordingly, the unrecognised occurrence of a fast reacting Si-containing product may explain the temperature independency of Si concentration. However, we have shown that a predominant effect of this process over a control by silicate dissolution was very uncertain, based on geochemical modelling, mineralogical observations, and finally reinforced by statistical analysis of the data compared to silicate dissolution experiments as a function of pH. Alternatively, and perhaps more likely, the absence of a significant relationship between Si concentration and T may reflect the limited data available and the small temperature range. In addition, this lack may also stem from the use of T values of a mixed origin, from either direct measurement in soil samples using a portable temperature probe or from in situ temperature probes located thorough the field site.

Acknowledgements

This research was funded by the Lorraine regional authorities (France). The authors thank our technical staff (especially S. Bienaimée, L. Gelhaye, B. Pollier), who performed the chemical analysis of soil solutions, A.-M. Wall (UCD, Translation Service, INRA Jouy-en-Josas, France) for revising the English and Dr. P. Montpied for his help in statistics. The authors also thank Drs. S. P. Anderson, A. E. Blum, J. Chorover

and an anonymous reviewer for their constructive comments and criticisms. **[EO]**

References

AFES, 1992. Principaux sols d'Europe. Référentiel pédologique. INRA (Ed.), Paris.

Anbeek, C., 1993. The effect of natural weathering on dissolution rates. Geochim. Cosmochim. Acta 57, 4963–4975.

Anbeek, C., van Breemen, N., Meijer, E.L., van der Plas, L., 1994. The dissolution of naturally weathered feldspar and quartz. Geochim. Cosmochim. Acta 58, 4601–4613.

Augusto, L., Turpault, M.-P., Ranger, J., 2000. Impact of forest tree species on feldspar weathering rates. Geoderma 96, 215–237.

Barhisel, R.I, Bertsch, P.M., 1989. Chlorites and hydroxy-interlayered vermiculites and smectites. In: Dixon, J.B., Weed, S.B. (Eds.), Mineral in Soil Environments. SSSA, Madison, WI, pp. 729–788.

Bennett, P.C., Casey, W., 1994. Chemistry and mechanisms of low-temperature dissolution of silicates by organic acids. In: Pittman, E.D., Lewan, M.D. (Eds.), Organic Acids in Geological Processes. Springer-Verlag, Berlin, Germany, pp. 162–200.

Bergelin, A., van Hees, P.A.W., Wahlberg, O., Lumdström, U.S., 2000. The acid–base properties of high and low molecular weight organic acids in soil solutions of podzolic soils. Geoderma 94, 223–235.

Berggren, D., Mulder, J., 1995. The role of organic matter in controlling aluminium solubility in acidic mineral soil horizons. Geochim. Cosmochim. Acta 59, 4167–4180.

Bloom, P.R., McBride, M.B., Weaver, R.M., 1979. Aluminum organic matter in acid soils: buffering and solution aluminum activity. Soil Sci. Soc. Am. J. 48, 488–493.

Blum, A.E., Stillings, L.L., 1995. Feldspar dissolution kinetics. In: White, A.F., Brantley, S.L. (Eds.), Chemical Weathering Rates of Silicate Minerals. Reviews in Mineralogy, vol. 31. MSA, Washington, DC, pp. 291–351.

Boudot, J.-P., Merlet, D., Rouiller, J., Maitat, O., 1994. Validation of an experimental procedure for aluminium speciation in soil solutions and surface waters. Sci. Total Environ. 158, 237–252.

Boudot, J.P., Maitat, O., Merlet, D., Rouiller, J., 2000. Soil solutions and surface water analysis in two contrasted watersheds impacted by acid deposition, Vosges mountains, N.E. France: interpretation in terms of Al impact and nutrient imbalance. Chemosphere 41, 1419–1429.

Brantley, S.L., 1998. Surface area and porosity of primary silicate minerals. Mineral. Mag. 62A, 229–230.

Brantley, S.L., Blai, A.C., Cremeen, D.L., MacInnis, I., Darmody, R.G., 1993. Natural etching rates of feldspar and hornblende. Aquat. Sci. 55, 262–272.

Cronan, C.S., Walker, W.J., Bloom, P.R., 1986. Predicting aqueous aluminium concentrations in natural waters. Nature 324, 140–143.

Dalghren, R.A., Walker, W.J., 1993. Aluminum release rates from selected Spodosol Bs horizons: effect of pH and solid-phase aluminum pools. Geochim. Cosmochim. Acta 57, 57–66.

Dietzel, M., 2000. Dissolution of silicates and the stability of polysilicic acid. Geochim. Cosmochim. Acta 19, 3275–3281.

Dietzel, M., 2001. Formation and stability of polymeric Al–Si complexes. Proc. 11th Goldschmidt Conference. Lunar and Planetary Inst., Houston.

Drever, J.I., Stillings, L.L., 1997. The role of organic acids in mineral weathering. Colloids and Surface: A. Physicochemical and Engineering Aspects 120, 167–181.

Drever, J.I., Vance, G.F., 1994. Role of soil organic acids in mineral weathering processes. In: Pittman, E.D., Lewan, M.D. (Eds.), Organic Acids in Geological Processes. Springer-Verlag, Berlin, Germany, pp. 138–161.

Drever, J.I., Zobrist, J., 1992. Chemical weathering of silicate rocks as a function of elevation in the southern Swiss Alps. Geochim. Cosmochim. Acta 56, 3209–3216.

Driscoll, C.T., Lehtinen, M.D., Sullivan, T.J., 1994. Modeling of acid–base chemistry of organic solutes in Adirondack, New-York lakes. Water Resour. Res. 30, 297–306.

Ezzaïm, A., Turpault, M.-P., Ranger, J., 1997. Répartition des nutriments dans un sol brun acide développé sur tuf (Beaujolais, France). Conséquences pour l'évolution de la fertilité minérale à long terme. Ann. Sci. For. 54, 371–387.

Ezzaïm, A., Turpault, M.-P., Ranger, J., 1999a. Quantification of weathering processes in an acid brown soil developed from tuff (Beaujolais, France): Part I. Formation of weathered rind. Geoderma 87, 137–154.

Ezzaïm, A., Turpault, M.-P., Ranger, J., 1999b. Quantification of weathering processes in an acid brown soil developed from tuff (Beaujolais, France): Part II. Soil formation. Geoderma 87, 155–177.

Frogner, P., Schweda, P., 1998. Hornblende dissolution kinetics at 25 °C. Chem. Geol. 151, 169–179.

Gérard, F., Boudot, J.-P., Ranger, J., 2001. Consideration on the occurrence of the Al_{13} polycation in natural soil solutions and surface waters. Appl. Geochem. 16, 513–529.

Gérard, F., Franҫois, M., Ranger, J., 2002. Processes controlling silica concentration in leaching and capillary soil solutions of an acidic brown forest soil (Rhône, France). Geoderma 107, 197–226.

Giesler, R., Lundström, U.S., 1993. Soil solution chemistry: effects of bulking soil samples. Soil Sci. Soc. Am. J. 57, 1283–1288.

Giesler, R., Lundström, U.S., Grip, H., 1996. Comparison of soil solution chemistry assessment using zero-tension lysimeters or centrifugation. Eur. J. Soil Sci. 47, 395–405.

Havenkamp, R., Zammit, C., Bouraoui, F., 1998. Grizzly soil data base, http://www.lthe.hmg.inpg.fr/Grizzly/.

Hellmann, R., 1994. The albite–water system: Part I. The kinetics of dissolution as a function of pH at 100, 200, and 300 °C. Geochim. Cosmochim. Acta 58, 595–611.

Hochella, M.F., Banfield, J.F., 1995. Chemical weathering of silicates in nature: a microscopic perspectives with theoretical considerations. In: White, A.F., Brantley, S.L. (Eds.), Chemical Weathering Rates of Silicate Minerals. Reviews in Mineralogy, vol. 31. MSA, Washington, DC, pp. 352–406.

Hodson, M.E., 1999. Micropore surface area variation with grain size in unweathered alkali feldspars: implications for surface roughness and dissolution studies. Geochim. Cosmochim. Acta 62, 3429–3435.

Kalinowski, B.G., Schweda, P., 1996. Kinetics of muscovite, phlogopite and biotite dissolution and alteration at pH 1–4, room temperature. Geochim. Cosmochim. Acta 60, 367–385.

Lasaga, A.C., 1995. Fundamental approaches in describing mineral dissolution and precipitation rates. In: White, A.F., Brantley, S.L. (Eds.), Chemical Weathering Rates of Silicate Minerals. Reviews in Mineralogy, vol. 31. MSA, Washington, DC, pp. 173–233.

Lundström, U., Öhman, L.O., 1990. Dissolution of feldspars in the presence of natural solutes. J. Soil Sci. 41, 359–369.

Lumsdon, D.G., Farmer, V.C., 1995. Solubility characteristics of proto-imogolite sols: how silicic acid can de-toxify aluminum solutions. Eur. J. Soil Sci. 46, 179–186.

Maitat, O., Boudot, J.-P., Merlet, D., Rouiller, J., 2000. Aluminium chemistry in two contrasted acid forest soils and headwater streams impacted by acid deposition, Vosges mountains, N.E. France. Water Air Soil Pollut. 117, 217–243.

Marques, R., Ranger, J., 1997. Nutrient dynamics in a chronosequence of Douglas-fir (*Pseudotsuga menziesii* (Mirb.) Franco) stands on the Beaujolais Mounts (France): 1. Qualitative approach. For. Ecol. Manag. 91, 255–277.

Marques, R., Ranger, J., Gelhaye, D., Pollier, B., Ponette, Q., Gobert, O., 1996. Comparison of chemical composition of soil solutions collected by zero-tension plate lysimeters with those from ceramic cup lysimeters in a forest soil. Eur. J. Soil Sci. 47, 407–417.

Meybeck, M., 1986. Composition chimique des ruisseaux non pollués de France. Sci. Géol. Bull. 39, 3–77.

Monterroso, C., Macías, F., 1998. Evaluation of the test-mineral method for studying minesoil geochemistry. Soil Sci. Soc. Am. J. 62, 1741–1748.

Nagy, K.L., 1995. Dissolution and precipitation kinetics of sheet silicates. In: White, A.F., Brantley, S.L. (Eds.), Chemical Weathering Rates of Silicate Minerals. Reviews in Mineralogy, vol. 31. MSA, Washington, DC, pp. 173–233.

Nugent, M.A., Brantley, S.L., Pantano, C.G., Maurice, P.A., 1998. The influence of natural mineral coatings on feldspar weathering. Nature 395, 588–591.

Ochs, M., 1996. Influence of humified and non-humified natural organic compounds on mineral dissolution. Chem. Geol. 132, 119–124.

Paces, T., 1983. Rate constants of dissolution derived from the measurement of mass balance in hydrologic catchments. Geochim. Cosmochim. Acta 47, 1855–1863.

Parkhurst, D.L., Appelo, C.A.J., 1999. User's guide to PHREEQC (Version 2). U.S. Geol. Surv., Water Resour. Inv. Rep. 95-4227.

Ranger, J., Marques, R., Colin-Belgrand, M., Flammang, N., 1995. The dynamics of biomass and nutrient accumulation in a Douglas-fir (*Pseudotsuga menziesii* Franco) stand studied using a chronosequence approach. For. Ecol. Manag. 72, 167–183.

Ranger, J., Marques, R., Jussy, J.-H., 2001. Forest dynamics during stand development assessed by lysimeter and centrifuge solutions. For. Ecol. Manag. 144, 129–145.

Raulund-Rasmussen, K., Borgaard, O.K., Hansen, H.C.B., Olsson, M., 1998. Effect of natural organic soil solutes on weathering rates of soil minerals. Eur. J. Soil Sci. 49, 397–406.

Schecher, W.D., Driscoll, C.T., 1995. ALCHEMI: a chemical equilibrium model to assess the acid–base chemistry and speciation of aluminum in dilute solutions. In: Leoppart, R.H., Schwab, A.P., Goldberg, S. (Eds.), Chemical Equilibrium and Reaction Models. SSSA Special Publication, vol. 42, pp. 325–356.

Simonsson, M., Berggren, D., 1998. Aluminium solubility related to secondary phases in upper B horizons with spodic characteristics. Eur. J. Soil Sci. 49, 317–326.

Steefel, C.I., van Cappellen, P., Nagy, K.L., Lasaga, A.C., 1990. Modeling water–rock interactions in the surficial environment: the role of precursors, nucleation, and Ostwald ripening. Chem. Geol. 84, 322–325.

Stillings, L.L., Drever, J.I., Brantley, S.L., Sun, Y., Oxburgh, R., 1996. Rates of feldspar dissolution at pH 3–7 with 0–8 mM oxalic acid. Chem. Geol. 132, 79–89.

Su, C., Harsh, J.B., Boyle, J.S., 1995. Solubility of hydroxy-aluminum interlayers and imogolite in a spodosol. Soil Sci. Soc. Am. J. 59, 373–379.

Sverdrup, H., Warfvinge, P., 1995. Estimating field weathering rates using laboratory kinetics. In: White, A.F., Brantley, S.L. (Eds.), Chemical Weathering Rates of Silicate Minerals. Reviews in Mineralogy, vol. 31. MSA, Washington, DC, pp. 485–541.

Swoboda-Colberg, N., Drever, J., 1993. Mineral dissolution rates in plot-scale field and laboratory experiments. Chem. Geol. 105, 51–69.

Tardy, Y., Fritz, B., 1981. An ideal solid solution model for calculating solubility of clay minerals. Clay Miner. 16, 361–373.

USDA, 1998. Keys for Soil Taxonomy, 8th ed. Soil Conservation Service, Pocahontas Press, Blacksburg, Virginia, USA.

van Hees, P.A.W., Lundström, U.S., Giesler, R., 2000. Low molecular weight organic acids and their Al-complexes in soil solution-composition, distribution and seasonal variation in three podzolized soils. Geoderma 94, 173–200.

van Hees, P.A.W., Tipping, E., Lundström, U.S., 2001. Aluminium speciation in forest soil solution—modelling the contribution of low molecular weight organic acids. Sci. Total Environ. 278, 215–229.

Wada, K., 1989. Allophane and imogolite. In: Dixon, J.B., Weed, S.B. (Eds.), Mineral in Soil Environments. SSSA, Madison, WI, pp. 1051–1087.

Webster, R., 2001. Statistics to support soil research and their presentation. Eur. J. Soil Sci. 52, 331–340.

Welch, S.A., Ullman, W.J., 1993. The effect of organic acids on plagioclase dissolution rates and stoechiometry. Geochim. Cosmochim. Acta 57, 2725–2736.

Welch, S.A., Ullman, W.J., 1996. Feldspar dissolution in acidic and organic solutions: compositional and pH dependence of dissolution rate. Geochim. Cosmochim. Acta 60, 2939–2948.

White, A.F., 1995. Chemical weathering rates of silicate minerals in soils. In: White, A.F., Brantley, S.L. (Eds.), Chemical Weathering Rates of Silicate Minerals. Reviews in Mineralogy, vol. 31. MSA, Washington, DC, pp. 407–459.

White, A.F., Blum, A.E., 1995. Effects of climate on chemical weathering in watersheds. Geochim. Cosmochim. Acta 59, 1729–1747.

White, A.F., Blum, A.E., Schulz, M., Bullen, T.D., Harden, J.W., Peterson, M.L., 1996. Chemical weathering rates of a soil chronosequence on granitic alluvium: I. Quantification of mineralog-

ical and surface area changes and calculation of primary silicate reaction rates. Geochim. Cosmochim. Acta 60, 2533–2550.

White, A.F., Blum, A.E., Bullen, T.D., Vivit, D.V., Schulz, M., Fitzpatrick, J., 1999. The effect of temperature on experimental and natural chemical weathering rates of granitoid rocks. Geochim. Cosmochim. Acta 63, 3277–3291.

White, A.F., Bullen, T.D., Schulz, M., Blum, A.E., Huntington, T.G., Peters, N.E., 2001. Differential rates of feldspar weathering in granitic regoliths. Geochim. Cosmochim. Acta 65, 847–869.

Xu, S., Harsh, J.B., 1993. Labile and nonlabile aqueous silica in acid solutions, relation to the colloidal fraction. Soil Sci. Soc. Am. J. 57, 1271–1277.

Zabowski, D., Ugolini, F.C., 1990. Lysimeter and centrifuge soil solutions: Seasonal differences between methods. Soil Sci. Soc. Am. J. 54, 1130–1135.

Zhang, H., Bloom, P.R., 1999. Dissolution kinetics of hornblende in organic acid solutions. Soil Sci. Soc. Am. J. 63, 815–822.

Zysset, M., Blaser, P., Luster, J., Gehring, A.U., 1999. Aluminum solubility control in different horizons of a podzol. Soil Sci. Soc. Am. J. 63, 1106–1115.